On Optimal Control Problems in Radiative Transfer

Michael Herty* **Rene Pinnau†** **Mohammed Seaïd‡**

October 10, 2005

Abstract

Optimal control problems for the radiative transfer equation are introduced and formulated. We consider as control variable a source term in the radiative transfer equation. Necessary and sufficient optimality conditions are derived and discussed. Numerical methods for the model equation and its adjoint are presented. Especially, the discrete ordinates method and finite volume discretization are formulated for two-dimensional problems. Computational results based on a steepest descent method are given for two test examples underlining the feasibility of our approach.

Keywords. Radiative transfer, Optimal control, First–Order Optimality, Discrete ordinates, S_N-equations, Iterative methods.

1 Introduction

During the last years optimal control and inverse problems for radiative heat transfer gained considerable attention in many fields of application, e.g. the cooling of glass, gas turbine combustion chambers or combustion in car engines [4, 23, 17, 16, 15]. These pose several challenging problems from the simulation point of view and even more challenging concerning the optimization, which have to be encountered by engineers and applied mathematicians. The reason is the high numerical complexity of the model equations which are given by the radiative heat transfer system for the radiative intensity. This led to the development of a whole hierarchy of approximative equations, ranging from moment expansion to diffusive type models, like the SP_N–systems [10, 9].

Due to the high dimensionality of the phase space of the discretized radiative transfer equation, most optimization approaches are based on approximate models coupled with a heat equation. These approaches allow to compute optimal controls at reasonable numerical costs. Nevertheless, there are applications in which one needs the detailed knowledge of the radiative intensity, like strongly scattering or optically thin media [14]. Then, the mentioned approximate models are no longer appropriate and one has to go back to the full radiative transfer equation (RTE). In this paper we will introduce and discuss optimal control problems for the multidimensional RTE including scattering.

Especially, we develop a numerical study for optimal control problems of tracking–type in radiative transfer where the cost functionals have the form

$$\mathcal{F}(R,Q) := \frac{\alpha_1}{2}\int_D \left(R-\bar{R}\right)^2 d\mathbf{x} + \frac{\alpha_2}{2}\int_D \left(Q-\bar{Q}\right)^2 d\mathbf{x}.$$

*Fachbereich Mathematik, Technische Universität Kaiserslautern, D–67663 Kaiserslautern, Germany (herty@rhrk.uni-kl.de)

†Fachbereich Mathematik, Technische Universität Kaiserslautern, D–67663 Kaiserslautern, Germany (pinnau@mathematik.uni-kl.de)

‡Fachbereich Mathematik, Technische Universität Kaiserslautern, D–67663 Kaiserslautern, Germany (seaid@mathematik.uni-kl.de)

Here, $R(\mathbf{x}) := \int_{S^d} \mathrm{I}(\omega.\mathbf{x})d\omega$ is the mean intensity and the radiative intensity I is given as the solution of the RTE. The variable of interest to be controlled is the source term Q, which can be interpreted as a gain or loss of radiant energy deployed by external forces.

Using the adjoint calculus we derive the first–order optimality condition and prove the existence of an optimal control. We use this first–order derivative information to devise a gradient method for the numerical optimization.

The paper is organized as follows. In the remainder of this section we recall the RTE used in the current work. Then, in Section 2 we formulate the optimal control problem associated with the considered RTE and derive the first–order optimality condition. We prove the existence of adjoint states and deduce the existence of an optimal control. In Section 3 we describe the steepest descent method and give an appropriate discretization for the optimal control problem. We present two numerical examples, source inversion and edging, in Section 4, which underline the feasibility of our approach.

1.1 The Radiative Transfer Equation

Radiative transfer equations can be written in general form [14, 13] as

$$\forall\ \nu > \nu_0 : \quad \frac{1}{c}\frac{\partial \mathrm{I}}{\partial t} + \omega \cdot \nabla \mathrm{I} + (\sigma + \kappa)\mathrm{I} = \frac{\sigma}{4\pi}\int_{S^d} \mathrm{I} d\omega + \kappa B(\theta, \nu), \tag{1.1}$$

where $\mathrm{I}(t, \nu, \omega, \mathbf{x})$ is the spectral intensity at time t, in position $\mathbf{x}$, within frequency ν and propagating along direction ω with a speed c. In (1.1), S^d denotes the unit sphere in $\mathbb{R}^d$, θ is the temperature, $\kappa = \kappa(\nu, \mathbf{x})$ is the absorption coefficient, $\sigma = \sigma(\nu, \mathbf{x})$ is the scattering coefficient, ν_0 is the upper bound of opaque band of the optical spectrum where radiation is completely absorbed, and $B(\theta, \nu)$ is the spectral intensity of the black-body radiation given by the Planck function

$$B(\theta, \nu) = \frac{2h\nu^3}{c_0^2}\left(e^{h\nu/k\theta} - 1\right)^{-1}, \tag{1.2}$$

where h, k and c_0 are Planck's constant, Boltzmann's constant and the speed of radiation propagation in vacuum, respectively, compare [13] for further physical details. For mathematical aspects of the radiative transfer equation and related issues see for instance [14]. We note that isotropic scattering media has been considered in (1.1) however, all the results presented in this paper can be straightforwardly extended to radiative transfer problems in non-isotropic scattering media.

The equations (1.1) are solved subject to the boundary condition

$$\mathrm{I}(t, \nu, \omega, \mathbf{x}) = \varrho(\mathbf{n} \cdot \omega)\mathrm{I}(t, \nu, \omega', \mathbf{x}) + (1 - \varrho(\mathbf{n} \cdot \omega))\, B(\theta_b, \nu), \quad \mathbf{n} \cdot \omega < 0, \tag{1.3}$$

where $\varrho \in [0, 1]$ is the reflectivity: $\varrho = 1$ for total reflection and $\varrho = 0$ for Dirichlet type boundary conditions. The temperature θ_b is a fixed boundary function, $\mathbf{n}$ is the outward normal on the boundary and $\omega' = \omega - 2(\mathbf{n} \cdot \omega)\mathbf{n}$ is the specular reflection of ω on the boundary. Initial condition is supplied to (1.1) as

$$\mathrm{I}(0, \nu, \omega, \mathbf{x}) = \mathrm{I}_0(\nu, \omega, \mathbf{x}), \tag{1.4}$$

with $\mathrm{I}_0(\nu, \omega, \mathbf{x})$ is a given function. For sake of simplicity, we shall consider the following radiative transfer model

$$\begin{aligned} \omega \cdot \nabla \mathrm{I} + (\sigma + \kappa)\mathrm{I} &= \frac{\sigma}{4\pi}\int_{S^d} \mathrm{I} d\omega + Q, \\ \mathrm{I}(\omega, \mathbf{x}) &= A, \qquad \mathbf{n} \cdot \omega < 0, \end{aligned} \tag{1.5}$$

where Q is the source term and A is a given boundary data.

Even so we assume severe simplifications, these equations are still reasonable in many applications, e.g. when dealing with grey medium and if the mean free path of the radiation is small compared to a characteristic length.

2 Optimal Control Problems in Radiative Transfer

In this section we give the precise mathematical setting of the optimal control problem and derive the first–order optimality conditions. Especially, we prove the existence of an unique optimal control. The ideas follow results of [7]. However, the considered function spaces as well as in the additionally treatment of optimal control problems is new.

Results on optimal control problems in the one-dimensional case are reported in [1]. In contrast to [1], we deal with multi–dimensional problems and distributed controls, but we do neglect heat transfer.

Different optimal control problems related to heat transfer are also discussed in [12].

2.1 The Optimal Control Problem

We consider an optimal control problem for a general objective function of tracking type (2.2). Then, we derive the first order optimality conditions and give existence and uniqueness results for the optimality system.

In the following, we assume that $\mathbf{x} \in D \subset \mathbb{R}^d$, $d = 2$ or 3. To avoid technical difficulties we assume that D is a bounded domain with Lipschitz boundary. We introduce a convex, tracking-type objective function of type depending on the mean intensity (also called "radiosity")

$$R(\mathbf{x}) := \int_{S^d} \mathrm{I}(\mathbf{x}, \omega) d\omega. \tag{2.1}$$

Furthermore, we denote distributed control by $Q(\mathbf{x})$ and we define the functional $\mathcal{F}$ as

$$\mathcal{F}(R, Q) := \frac{\alpha_1}{2} \int_D \left(R - \bar{R}\right)^2 d\mathbf{x} + \frac{\alpha_2}{2} \int_D \left(Q - \bar{Q}\right)^2 d\mathbf{x}, \tag{2.2}$$

with positive constants α_1, α_2 and given (desired) states and controls $\bar{R}$ and $\bar{Q}$, respectively.

The general optimal control problem reads

$$\min_{R,Q} \mathcal{F}(R, Q) \text{ subject to (1.5) and (2.1).} \tag{2.3}$$

with function spaces for R and Q defined below.

Formally, the partial differential equation (2.4) for the adjoint function $J(\omega, \mathbf{x})$ is given by

$$\begin{aligned} -\omega \cdot \nabla J(\omega, \mathbf{x}) + (\sigma + \kappa) J(\omega, \mathbf{x}) &= \frac{\sigma}{4\pi} \int_{S^d} J(\omega, \mathbf{x}) d\omega + \alpha_1 \left(R(\mathbf{x}) - \bar{R}(\mathbf{x})\right), \\ J(\omega, \mathbf{x}) &= 0, \qquad \mathbf{n} \cdot \omega > 0. \end{aligned} \tag{2.4}$$

and the gradient equation (or optimality condition) is given by

$$\alpha_2 \left(Q(\mathbf{x}) - \bar{Q}(\mathbf{x})\right) + \int_{S^d} J(\omega, \mathbf{x}) d\omega = 0. \tag{2.5}$$

2.2 Adjoint Calculus

We now give a rigorous derivation of the adjoint and gradient equation. First and as in [7], we *reformulate* the state equation (1.5) of the optimal control problem: Let D be a bounded domain and let A be constant boundary data for ingoing directions ω. For a fixed $\mathbf{x} \in D$ and a fixed direction $\omega \in S^d$ we denote by $p(\omega) \in \partial D$ the point, where the direction ω meets the boundary of D for the first time and such that $\overline{\mathbf{x}p(\omega)}$ is parallel to ω, see Figure 2.1.

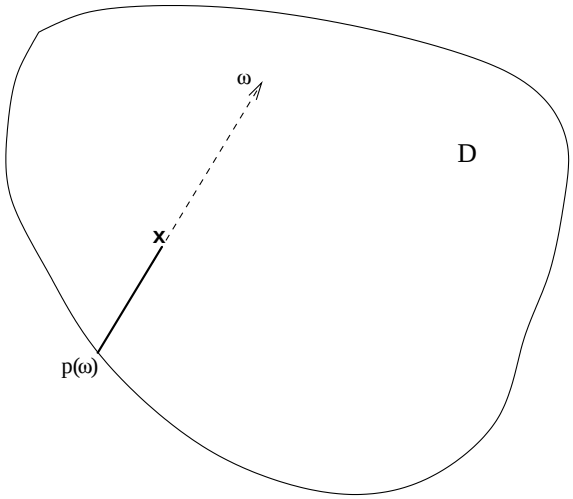

Figure 2.1: Domain D and the points $\mathbf{x}$ and $p(\omega)$ for the two-dimensional problem.

For fixed $(\omega, \mathbf{x}) \in S^d \times D$ we integrate (1.5) along the line–segment $\overline{p(\omega)\mathbf{x}}$ and obtain an (implicit) equation for $R(\mathbf{x})$:

$$\begin{aligned} R(\mathbf{x}) &= A \int_{S^d} \exp\left(- \int_{p(\omega)}^{\mathbf{x}} (\sigma + \kappa) ds \right) d\omega + \\ &\quad \int_{S^d} \int_{p(\omega)}^{\mathbf{x}} \exp\left(- \int_{r}^{\mathbf{x}} (\sigma + \kappa) ds \right) \left(\frac{\sigma}{4\pi} R(r) + Q(r) \right) dr d\omega. \end{aligned} \tag{2.6a}$$

Note, that the integrals are path integrals along line–segments. Therefore, and if we assume σ and κ to be constant on D,

$$\int_{p(\omega)}^{\mathbf{x}} (\sigma + \kappa) ds = \|\mathbf{x} - p(\omega)\|_2 (\sigma + \kappa). \tag{2.7}$$

Moreover, there exists a coordinate transformation, such that the integrals in (2.6) can be given in Euclidean coordinates: Consider a fixed point $\mathbf{x}$ in the interior of D and a fixed direction $\omega \in S^d$. Then, a parametrization of the line–segment $\overline{p(\omega)\mathbf{x}}$ is given by

$$t \mapsto \gamma(t; \omega, x) = \mathbf{x} - t\omega, \ \gamma : [0, c_\omega] \longrightarrow \overline{p(\omega)\mathbf{x}},$$

for some constant c_ω. For each $\mathbf{y}$ in the interior of D and $\mathbf{y} \neq \mathbf{x}$, we find a unique pair (ω, t) such that

$$\gamma(\omega, t) = \mathbf{y} \text{ and } t \leq c_\omega.$$

Hence, the transformation $\Phi : \{(\omega, t) : \omega \in S^d, t \in [0, c_\omega]\} \to D$ is well–defined. The transformation formulas yield in the multi-dimensional case (see also [7])

$$d = 2 : \qquad \int_{S^2} \int_{p(\omega)}^{\mathbf{x}} F(r) dr d\omega = \int_D \frac{F(\mathbf{y})}{\|\mathbf{x} - \mathbf{y}\|_2} d\mathbf{y}, \tag{2.8}$$

$$d = 3 : \qquad \int_{S^3} \int_{p(\omega)}^{\mathbf{x}} F(r) dr d\omega = \int_D \frac{F(\mathbf{y})}{\|\mathbf{x} - \mathbf{y}\|_2^2} d\mathbf{y}. \tag{2.9}$$

Second, we prove some properties of the kernel of equation (2.6). Lemma 1 is similar to [7] and changed only to incorporate our the two–dimensional case and our boundary condition.

Lemma 1 *Let $d = 2$. Assume $\sigma, \kappa > 0$ to be constant on a bounded domain D. Define the kernel $k(x, y) : D \times D \to \mathbb{R}$ by*

$$k(\mathbf{x}, \mathbf{y}) = \sigma \frac{\exp\left(-(\sigma + \kappa)\|\mathbf{x} - \mathbf{y}\|_2\right)}{4\pi\|\mathbf{x} - \mathbf{y}\|_2}. \tag{2.10}$$

Then the following holds true.

(i) $k(\cdot, \mathbf{y}) \in L^1(D)$, $k(\mathbf{x}, \mathbf{y}) = k(\mathbf{y}, \mathbf{x})$ *and* $k \geq 0$.

(ii) The operator $K : L^p(D) \to L^p(D)$ given by

$$K(f)(\mathbf{x}) = \int_{S^d} \int_{p(\omega)}^{\mathbf{x}} \frac{\sigma}{4\pi} \exp\left(-\int_r^{\mathbf{x}} (\sigma + \kappa)\, ds\right) f(r) dr d\omega, \tag{2.11}$$

is well-defined for $1 \leq p < \infty$.

(iii) $\int_D K(f)(\mathbf{x})d\mathbf{x} = \int_D K(1)(\mathbf{x})f(\mathbf{x})d\mathbf{x}$ *for all* $f \in L^p(D), 1 \leq p < \infty$.

(iv) $\|K\|_{L^p(D),L^p(D)} \leq 1$ *for* $1 < p < \infty$ *and* $(I - K) : L^p(D) \to L^p(D)$ *is an invertible operator.*

Proof.

Obviously, k is symmetric and non-negative. Using the coordinate transformation introduced above, we see, that $k(\cdot, \mathbf{y}) \in L^1(D)$. Next, we prove that K maps $L^p(D)$ to $L^p(D)$. Consider $f \in L^1(D)$, then by Fubini's theorem

$$\begin{aligned} \int_D |K(f)|(\mathbf{x})d\mathbf{x} &= \int_{D\times D} k(\mathbf{x}, \mathbf{y})|f(\mathbf{y})|d\mathbf{y}d\mathbf{x}, \\ &= \int_D |f(\mathbf{y})| \int_D k(\mathbf{x}, \mathbf{y})d\mathbf{x}d\mathbf{y} < \infty. \end{aligned} \tag{2.12}$$

Equation (2.12) also reveals property (iii). Further, for $f \in L^p(D)$, $1 < p < \infty$ we obtain by Hölder's inequality for $1/p + 1/q = 1$:

$$\begin{aligned} \int_D |K(f)(\mathbf{x})|^p d\mathbf{x} &= \int_D \left(\int_D k(\mathbf{x}, \mathbf{y})^{\frac{1}{p}+\frac{1}{q}} |f(\mathbf{y})|d\mathbf{y}\right)^p d\mathbf{x} \\ &\leq \int_D \left(\int_D k(\mathbf{x}, \mathbf{y})|f(y)|^p d\mathbf{y}\right) \left(\int_D k(\mathbf{x}, \mathbf{y})d\mathbf{y}\right)^{p/q} d\mathbf{x} \\ &\leq c_2^{p/q} \int_D K(|f|^p)(\mathbf{x})d\mathbf{x} \\ &\leq \int_D |f(\mathbf{y})|^p \int_D k(\mathbf{x}, \mathbf{y})d\mathbf{x}d\mathbf{y} \\ &\leq c_2^{p/q+1} \|f\|^p_{L^p(D)} < \infty, \end{aligned}$$

where $c_2 = \int_D k(\mathbf{x}, \mathbf{y})d\mathbf{y}$. The above calculation yields $\|K\|_{L^p(D),L^p(D)} \leq 1$, once we proved

that $c_2 \leq 1$.

$$\begin{aligned}
\int_D k(\mathbf{x},\mathbf{y})d\mathbf{y} &= \int_D \frac{\sigma}{4\pi}\frac{\exp(-\sigma\|\mathbf{x}-\mathbf{y}\|_2)}{\|\mathbf{x}-\mathbf{y}\|}\exp(-\kappa\|\mathbf{x}-\mathbf{y}\|_2)d\mathbf{y} \\
&\leq \int_D \frac{\sigma}{4\pi}\frac{\exp(-\sigma\|\mathbf{x}-\mathbf{y}\|_2)}{\|\mathbf{x}-\mathbf{y}\|_2}d\mathbf{y} \\
&= \int_{S^2}\frac{1}{4\pi}\int_{p(\omega)}^{\mathbf{x}}\exp(-\sigma\|\mathbf{x}-r\|_2)\sigma dr d\omega \\
&= \int_{S^2}\frac{1}{4\pi}\exp\left(-\sigma\|\mathbf{x}-r\|_2\right)|_{r=p(\omega)}^{r=\mathbf{x}}d\omega \\
&\leq \frac{1}{4\pi}\int_{S^2}1\, d\omega \\
&\leq \frac{1}{2}.
\end{aligned}$$

This finishes the proof.

Remark 1 *Lemma 1 remains true in the case $d = 3$, if we replace the kernel $k(\mathbf{x},\mathbf{y})$ by*

$$k(\mathbf{x},\mathbf{y}) = \sigma\frac{\exp(-(\sigma+\kappa)\|\mathbf{x}-\mathbf{y}\|_2)}{\|\mathbf{x}-\mathbf{y}\|_2^2}.$$

Then one obtains $c_2 \leq 1$ and again $\|K\|_{L^p(D),L^p(D)} \leq 1$.

Remark 2 *In fact, Lemma 1 is an existence theorem for equation (2.6). Indeed, let us rewrite (2.6) as*

$$R(\mathbf{x}) = c_1 + K(R)(\mathbf{x}) + K\left(\frac{4\pi}{\sigma}Q\right)(\mathbf{x}), \tag{2.13}$$

with the constant

$$c_1 := A\int_{S^d}\exp\left(-\int_{p(\omega)}^{\mathbf{x}}(\sigma+\kappa)ds\right)d\omega. \tag{2.14}$$

Then, for $Q \in L^p(D)$, we obtain from Lemma 1 the unique solution to (2.13) as

$$R = (Id-K)^{-1}\left(c_1 + K\left(\frac{4\pi}{\sigma}Q\right)(\mathbf{x})\right). \tag{2.15}$$

If $\sigma \in L^\infty(D)$, we consider the weighted L^p-space

$$L^p_\sigma(D) := \left\{f : \int_D f^p(\mathbf{y})\sigma(\mathbf{y})d\mathbf{y} < \infty\right\}$$

and define $K : L^p_\sigma \to L^p_\sigma$ to proceed analogously to Lemma 1. For our purposes the case σ and κ constant, is sufficient.

Finally and with all the previous remarks in mind, we can state the optimal control problem. Due to Remark 2 and Lemma 1, the following reformulation of the optimal control problem (2.3) is well–posed. Let $d = 2$ or 3 and $\bar{R}, \bar{Q} \in L^2(D)$ are given functions,

$$\min_{R,Q\in L^2(D)}\frac{\alpha_1}{2}\int_D\left(R(\mathbf{x})-\bar{R}(\mathbf{x})\right)^2 d\mathbf{x} + \frac{\alpha_2}{2}\int_D\left(Q(\mathbf{x})-\bar{Q}(\mathbf{x})\right)^2 d\mathbf{x}, \tag{2.16}$$

subject to

$$\begin{aligned} R(\mathbf{x}) &= A\int_{S^d}\exp\left(-\int_{p(\omega)}^{\mathbf{x}}(\sigma+\kappa)ds\right)d\omega + \\ &\quad \int_{S^d}\int_{p(\omega)}^{\mathbf{x}}\exp\left(-\int_{r}^{\mathbf{x}}(\sigma+\kappa)ds\right)\left(\frac{\sigma}{4\pi}R(r)+Q(r)\right)drd\omega. \end{aligned} \tag{2.17}$$

Now, we are able to derive the necessary optimality conditions for (2.16). Let,

$$\mathcal{H}(R,Q) := (\mathbb{I}_d - K)R - c_1 - K\left(\frac{4\pi}{\sigma}Q\right) : L^2(D)\times L^2(D)\to L^2(D),$$

where $\mathbb{I}_d$ denotes the identity matrix in $\mathbb{R}^d$. Obviously, for all $R, Q \in L^2(D)$, the operator $\mathcal{H}'$ is linear and bounded, i.e.,

$$\mathcal{H}'(R,Q) \in L\left(L^2(D)\times L^2(D); L^2(D)\right).$$

Moreover, for any $f \in L^2(D)$ and all $R, Q \in L^2(D)$ the pre-image

$$(R_f, Q_f) = \left(f, -\frac{\sigma}{4\pi}f\right)$$

satisfies

$$\mathcal{H}'(R,Q)[R_f, Q_f] = f.$$

Here and from now $\mathbf{A}[x]$ represent the application of the linear operator $\mathbf{A}$ to x. The above calculations show, that $\mathcal{H}'$ is a surjective operator defined on $L^2(D)\times L^2(D)$. Therefore, we can apply the Lagrange Multiplier Theorem to derive the necessary optimality conditions. To be more precise, due to [11][Theorem 1, p243], there exists a function $\lambda^* \in L^2(D)^*$, which we identify with $\lambda \in L^2(D)$, such that the necessary first–order optimality conditions (2.18) are satisfied in a local minimum (R_0, Q_0). Moreover, since $\mathcal{F}$ is convex, these conditions are also sufficient.

$$\mathcal{F}'(R_0,Q_0)[R,Q] - \int_D \lambda(\mathbf{x})\mathcal{H}'(R_0,Q_0)[R,Q](\mathbf{x})d\mathbf{x} = 0, \quad \forall\, R, Q \in L^2(D), \tag{2.18a}$$

$$\mathcal{H}(R_0,Q_0) = 0, \quad a.e. \quad \mathbf{x}\in D. \tag{2.18b}$$

Next, we verify the formal calculations by further discussion of properties of the first order optimality system (2.18).

Using the variational lemma we deduce from (2.18a)

$$\alpha_1\left(R_0 - \bar{R}\right) - (Id - K^*)\lambda = 0, \quad a.e. \quad \mathbf{x}\in D, \tag{2.19a}$$

$$\alpha_2\left(Q_0 - \bar{Q}\right) + \frac{4\pi}{\sigma}K^*\lambda = 0, \quad a.e. \quad \mathbf{x}\in D, \tag{2.19b}$$

where $K^* : L^2(D)\to L^2(D)$ is the adjoint operator to K. K is self–adjoint, since in Euclidean coordinates we have:

$$\begin{aligned} \int_D g(\mathbf{x})K(f)(\mathbf{x})d\mathbf{x} &= \int_D\int_D g(\mathbf{x})k(\mathbf{x},\mathbf{y})f(\mathbf{y})d\mathbf{y}d\mathbf{x}, \\ &= \int_D\int_D g(\mathbf{x})k(\mathbf{y},\mathbf{x})f(\mathbf{y})d\mathbf{y}d\mathbf{x}, \\ &= \int_D K(g)(\mathbf{y})f(\mathbf{y})d\mathbf{y}. \end{aligned}$$

Furthermore, since λ satisfies the above system we conclude that there exists a function

$$P(\mathbf{x}) := \frac{4\pi}{\sigma} K^* \left(\lambda(\mathbf{x})\right) \in L^2(D),$$

which satisfies

$$\begin{aligned} \alpha_1 \frac{4\pi}{\sigma} K^* \left(R_0 - \bar{R}\right) - (\mathbb{I}_d - K^*)P &= 0, \quad a.e. \quad \mathbf{x} \in D, && \text{(2.20a)} \\ \alpha_2 \left(Q_0 - \bar{Q}\right) + P &= 0, \quad a.e. \quad \mathbf{x} \in D. && \text{(2.20b)} \end{aligned}$$

The condition (2.20) is necessary for optimality but not sufficient, since in general K^* is not invertible. An equation for P will be used to justify the formal computations in the beginning. From the first equation in (2.20) we derive the equivalent reformulation in Euclidean coordinates

$$P(\mathbf{x}) = \int_D k(\mathbf{x}, \mathbf{y}) \left(P(\mathbf{y}) + \alpha_1 \frac{4\pi}{\sigma} \left(R_0(\mathbf{y}) - \bar{R}(\mathbf{y})\right) \right) d\mathbf{y}. \tag{2.21}$$

Now, we justify the formal calculations in the first section: For fixed $\omega \in S^d$ denote by $p^*(\omega)$ the point on ∂D where the direction ω **leaves** D. In contrast to the previous discussion we consider path–integrals along the line–segment $\overline{\mathbf{x}p^*(\omega)}$ and its parametrization

$$t \mapsto \gamma^*(t; \mathbf{x}, \omega) := \mathbf{x} + t\omega, \ \gamma : [0, c^*_\omega] \longrightarrow \overline{\mathbf{x}p^*(\omega)}$$

for some constant c^*_ω and fixed $\omega \in S^d$, see Figure 2.2. Again, for each $\mathbf{y} \neq \mathbf{x}$ in the interior of D we find a unique (t, ω) such that

$$\gamma^*(t, \omega) = \mathbf{y}$$

and $t \leq c^*_\omega$. This defines a transformation Φ^* from D to $\{(t, \omega) : \omega \in S^d, 0 \leq t \leq c^*_\omega\}$.

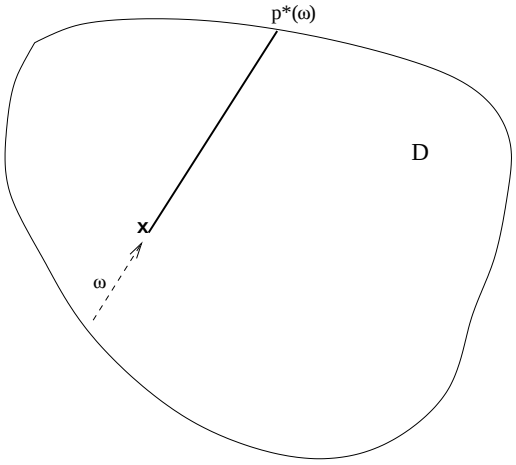

Figure 2.2: Domain D and the points $\mathbf{x}$ and $p^*(\omega)$ for the two-dimensional problem

Applying the transformation Φ^* to (2.21) we obtain

$$P(\mathbf{x}) = \int_{S^d} \int_{p^*(\omega)}^{\mathbf{x}} \exp\left(- \int_r^{\mathbf{x}} (\sigma + \kappa) ds \right) \left(\frac{\sigma}{4\pi} P(r) + \alpha_1 \left(R_0(r) - \bar{R}(r)\right) \right) dr d\omega. \tag{2.22}$$

Equation (2.22) is the reformulation of

$$\begin{aligned} -\omega \cdot \nabla \mathrm{J}(\omega, \mathbf{x}) + (\sigma + \kappa)\mathrm{J}(\omega, \mathbf{x}) &= \frac{\sigma}{4\pi} \int_{S^d} \mathrm{J}(\omega, \mathbf{x}) d\omega + \alpha_1 \left(R_0(\mathbf{x}) - \bar{R}(\mathbf{x})\right), && \text{(2.23a)} \\ \mathrm{J}(\omega, \mathbf{x}) &= 0, \qquad \mathbf{n} \cdot \omega > 0, && \text{(2.23b)} \end{aligned}$$

provided that

$$P(\mathbf{x}) = \int_{S^d} J(\omega, \mathbf{x}) d\omega.$$

Here, $J(\mathbf{x}, \omega)$ is the solution to equation (2.23). This follows from (2.24), (2.22), Remark 3 (see below) and the definition of Φ^*.

Remark 3 *Using the definitions above, we derive for a differentiable function F and a fixed direction ω, the following equation (2.24).*

$$\int_{p^*(\omega)}^{\mathbf{x}} -\omega \cdot \nabla F(s, \omega) ds = F(\mathbf{x}, \omega) - F(p^*(\omega), \omega). \tag{2.24}$$

We summarize the calculations above as final result of this section.

Theorem 1 *Given a bounded domain $D \in \mathbb{R}^d$ with $d = 2$ or 3. Let positive constants α_1, α_2 and functions $\bar{R}, \bar{Q} \in L^2(D)$ be given. Consider the optimal control problem (2.16).*

Then, there exists a function $\lambda \in L^2(D)$, such that the necessary and sufficient first order optimality conditions for (2.16) are as follows:

$$\alpha_1 \left(R_0 - \bar{R}\right) - (\mathbb{I}_d - K^*)\lambda = 0, \quad a.e. \quad \mathbf{x} \in D, \tag{2.25a}$$

$$\alpha_2 \left(Q_0 - \bar{Q}\right) + \frac{4\pi}{\sigma} K^* \lambda = 0, \quad a.e. \quad \mathbf{x} \in D, \tag{2.25b}$$

$$(\mathbb{I}_d - K) R(\mathbf{x}) = \left(c_1 + K\left(\frac{4\pi}{\sigma} Q\right)(\mathbf{x})\right), \quad a.e. \quad \mathbf{x} \in D. \tag{2.25c}$$

Here, the operator K is defined in (2.11) and the constant c_1 is given by (2.14).

A direct consequence is the following result.

Theorem 2 *There exists a unique minimizer $(R, Q) \in L^2(D)$ of the optimization problem (2.3).*

As seen in the calculations the formal adjoint equation to (1.5) are given by (2.23).

3 Solution Procedure

In this section, we present the numerical procedure used to solve the optimal control problem (2.3). We use a gradient method based on the formal state and adjoint equations derived in the previous section. We discretize the governing equations in space and angular directions. A different method is proposed by Kelley *et.al.* in [3]. A gradient method applied to the problem results in the following steps:

1. Given an initial control $Q(\mathbf{x})$.
2. Loop until convergence:
   (a) Compute solution to the state equation and obtain $\mathrm{I}(\omega, \mathbf{x})$ by solving (1.5)
   (b) Compute solution to the adjoint equation and obtain $\mathrm{J}(\omega, \mathbf{x})$ by solving (2.4)
   (c) Compute the gradient $\nabla_Q \mathcal{F}$ by (2.5), i.e.,

$$\nabla_Q \mathcal{F}(\mathbf{x}) = \alpha_2 \left(Q(\mathbf{x}) - \bar{Q}(\mathbf{x})\right) + \int_{S^d} J(\omega, \mathbf{x}) d\omega \tag{3.1}$$

Table 3.1: Ordinates and weights used in the S_8 discretization.

m	μ_m	ξ_m	η_m	w_m
1	0.97097459	0.16912768	0.16912768	0.14613894
2	0.79878814	0.16912768	0.57735027	0.15983890
3	0.79878814	0.57735027	0.16912768	0.15983890
4	0.57735027	0.16912768	0.79878814	0.15983890
5	0.57735027	0.57735027	0.57735027	0.17334611
6	0.57735027	0.79878814	0.16912768	0.15983890
7	0.16912768	0.16912768	0.97097459	0.14613894
8	0.16912768	0.57735027	0.79878814	0.15983890
9	0.16912768	0.79878814	0.57735027	0.15983890
10	0.16912768	0.97097459	0.16912768	0.14613894

(d) Choose a steplength δ such that the sufficient decrease condition [21] for $\mathcal{F}$ is satisfied and update the control by

$$Q^{new}(\mathbf{x}) = Q^{old}(\mathbf{x}) - \delta \nabla_Q \mathcal{F}(\mathbf{x}), \qquad \forall\, \mathbf{x} \in D. \tag{3.2}$$

Note that, for the discrete problem, the control $Q(\mathbf{x})$ has to be replaced by its discrete values Q_{ij} at the gridpoints $\mathbf{x}_{ij}$. An iteration in the step 2 requires the solution of the radiative transfer equation and its associated adjoint problem. The gradient in (3.1) is approximate by a quotient difference whereas, the steplength δ is selected according to the Armijo technique. Details on steepest descent methods can be found in standard textbooks, see [21]. Other approaches to solve (2.3) are trust–region or SQP methods. We refer to the literature for a detailed discussion, see [22, 2, 6].

3.1 Fully Discrete Problem

In the present work, the angle and space variables are discretized using a discrete ordinates and finite volume method, respectively. For sake of brevity we shall formulate the methods only for the radiative transfer equation (1.5) and the adjoint equation (2.4) can be treated in similar manner. The outstanding aspect of discrete ordinates method is that such an integral is approximated by a low computational cost procedure, which is analogous to the Gauss-Legendre method. It consists of the substitution of the integral term in (1.5) with a weighted summation of the integrand at selected ordinates of the unit sphere. This method is sometimes referred to as the S_N approximation, where N represents the number of discrete values of direction cosines to be considered. In general, the total number of ordinate directions M in a set S_N is given by $M = N(N+2)/2$. The S_8 discretization is well designed for solving radiative transfer problem. For each direction ω_m of the quadrature, a specific weight w_m is associated with a set of three cosine angles μ_m, ξ_m and η_m in the direct Cartesian grid (x, y, z). The cosine angles and the weights for S_8 quadrature are listed in table 3.1. Other discrete S_N sets can be found in [14, 5]. For the two-dimensional Cartesian coordinates, the radiative transfer equation (1.5) can be expressed for each individual ordinate direction, m, as

$$\mu_m \frac{\partial \mathrm{I}_m}{\partial x} + \xi_m \frac{\partial \mathrm{I}_m}{\partial y} + (\sigma + \kappa)\mathrm{I}_m = \frac{\sigma}{4\pi} \sum_{k=1}^{M} w_k \mathrm{I}_k + Q, \qquad m = 1, 2, \ldots, M, \tag{3.3}$$

where I_m denotes the radiant intensity at the discrete ordinate ω_m. Next, the finite volume technique is applied, which consists of the integration of the S_N-equation (3.3) over a control volume such that shown in Figure 3.1. The result is an equation relating the value of an arbitrary function ψ at the nodal point, $\psi_{i+\frac{1}{2}j+\frac{1}{2}}$, to the value at each adjacent line ψ_{ij}, ψ_{i+1j}, ψ_{ij+1} and ψ_{i+1j+1}. The fully discrete problem corresponding to the equation (1.5) is written as

$$\mu_m \frac{\mathrm{I}_{m,i+1j} - \mathrm{I}_{m,ij}}{(\Delta x)_{i+\frac{1}{2}}} + \xi_m \frac{\mathrm{I}_{m,ij+1} - \mathrm{I}_{m,ij}}{(\Delta y)_{j+\frac{1}{2}}} + \left(\sigma_{i+\frac{1}{2}j+\frac{1}{2}} + \kappa_{i+\frac{1}{2}j+\frac{1}{2}}\right)\mathrm{I}_{m,i+\frac{1}{2}j+\frac{1}{2}} = \frac{\sigma_{i+\frac{1}{2}j+\frac{1}{2}}}{4\pi} \sum_{k=1}^{M} w_k \mathrm{I}_{k,i+\frac{1}{2}j+\frac{1}{2}} + Q_{i+\frac{1}{2}j+\frac{1}{2}}, \quad (3.4)$$

where the cell averages of a function ψ are given by

$$\begin{aligned} \psi_{i+1j} &= \frac{1}{(\Delta y)_{i+\frac{1}{2}}} \int_{y_j}^{y_{j+1}} \psi(x_i, y) dy, \\ \psi_{ij+1} &= \frac{1}{(\Delta x)_{j+\frac{1}{2}}} \int_{x_i}^{x_{i+1}} \psi(x, y_j) dx, \\ \psi_{ij} &= \frac{1}{(\Delta x)_{i+\frac{1}{2}} (\Delta y)_{j+\frac{1}{2}}} \int_{x_i}^{x_{i+1}} \int_{y_j}^{y_{j+1}} \psi(x, y) dx dy, \end{aligned} \quad (3.5)$$

The cell center and cell boundary function in the fluxes (3.5) are related to each other by a selected interpolation scheme. Here, we use the diamond difference method which consists of approximating the function values at the cell centers by the average of their values at the neighboring nodes. Thus, the function value of $\psi_{i+\frac{1}{2}j+\frac{1}{2}}$ at the cell center is simply approximated by a bilinear interpolation as

$$\psi_{i+\frac{1}{2}j+\frac{1}{2}} = \frac{\psi_{ij} + \psi_{i+ij} + \psi_{ij+1} + \psi_{i+1j+1}}{4}. \quad (3.6)$$

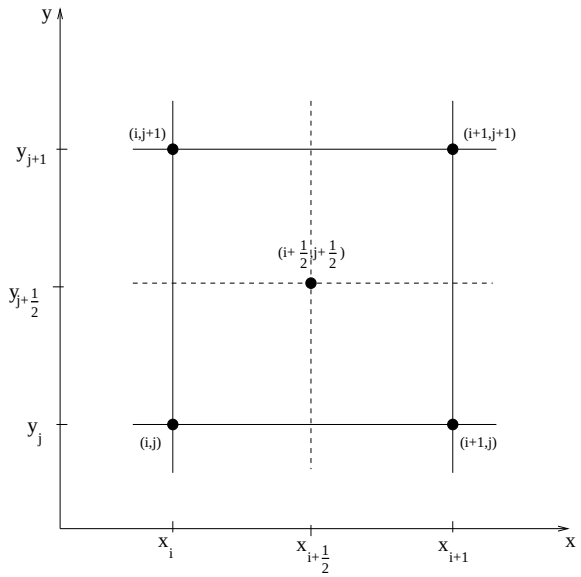

Figure 3.1: Spatial mesh and typical control volume.

With the introduction of the above interpolation relations into (3.4), the resulting fully discrete equations can be solved by proceeding in the direction of photon travel

on the spatial mesh, that is, sweeping away from the boundary conditions in the mesh. For problems involving scattering media or reflecting boundaries, the discrete ordinates equations are coupled and therefore have to be solved iteratively.

In order to formulate the equations (3.4) in a compact linear algebra form, we first define the matrix entries

$$\begin{aligned}
d_{m,i+\frac{1}{2}j+\frac{1}{2}} &:= \frac{|\mu_m|}{2(\Delta x)_{i+\frac{1}{2}}} + \frac{|\xi_m|}{2(\Delta y)_{j+\frac{1}{2}}} + \frac{\sigma_{i+\frac{1}{2}j+\frac{1}{2}} + \kappa_{i+\frac{1}{2}j+\frac{1}{2}}}{4}, \\
\bar{e}_{m,i+\frac{1}{2}j+\frac{1}{2}} &:= \frac{|\mu_m|}{2(\Delta x)_{i+\frac{1}{2}}} + \frac{-|\xi_m|}{2(\Delta y)_{j+\frac{1}{2}}} + \frac{\sigma_{i+\frac{1}{2}j+\frac{1}{2}} + \kappa_{i+\frac{1}{2}j+\frac{1}{2}}}{4}, \\
\underline{\mathrm{e}}_{l,i+\frac{1}{2}j+\frac{1}{2}} &:= \frac{-|\mu_m|}{2(\Delta x)_{i+\frac{1}{2}}} + \frac{|\xi_m|}{2(\Delta y)_{j+\frac{1}{2}}} + \frac{\sigma_{i+\frac{1}{2}j+\frac{1}{2}} + \kappa_{i+\frac{1}{2}j+\frac{1}{2}}}{4}, \\
e_{l,i+\frac{1}{2}j+\frac{1}{2}} &:= \frac{-|\mu_m|}{2(\Delta x)_{i+\frac{1}{2}}} + \frac{-|\xi_m|}{2(\Delta y)_{j+\frac{1}{2}}} + \frac{\sigma_{i+\frac{1}{2}j+\frac{1}{2}} + \kappa_{i+\frac{1}{2}j+\frac{1}{2}}}{4}.
\end{aligned}$$

Define the vectors

$$\boldsymbol{\Psi}_m \equiv \begin{pmatrix} \Psi_{m,0} \\ \vdots \\ \Psi_{l,Ny} \end{pmatrix} \in \mathbb{R}^{(Nx+1)(Ny+1)}, \quad \text{with} \quad \Psi_{m,j} \equiv \begin{pmatrix} \mathrm{I}_{m,0j} \\ \vdots \\ \mathrm{I}_{l,Nxj} \end{pmatrix} \in \mathbb{R}^{Nx+1},$$

$$\boldsymbol{\Phi} \equiv \begin{pmatrix} \Phi_{\frac{1}{2}} \\ \vdots \\ \Phi_{Ny-\frac{1}{2}} \end{pmatrix} \in \mathbb{R}^{NxNy}, \quad \text{with} \quad \Phi_{j-\frac{1}{2}} \equiv \begin{pmatrix} \phi_{\frac{1}{2}j-\frac{1}{2}} \\ \vdots \\ \phi_{Nx-\frac{1}{2}j-\frac{1}{2}} \end{pmatrix} \in \mathbb{R}^{Nx};$$

$$\text{and} \qquad \mathbf{Q}_m \equiv \begin{pmatrix} Q_{m,\frac{1}{2}} \\ \vdots \\ Q_{m,Ny-\frac{1}{2}} \end{pmatrix} \in \mathbb{R}^{NxNy}, \quad \text{with} \quad Q_{m,j-\frac{1}{2}} \equiv \begin{pmatrix} q_{m,\frac{1}{2}j-\frac{1}{2}} \\ \vdots \\ q_{m,Nx-\frac{1}{2}j-\frac{1}{2}} \end{pmatrix} \in \mathbb{R}^{Nx}.$$

Recall that the S_N-direction set used for the discrete ordinates formulation (3.3) avoid the zero component in a given direction ω_l. So, only one of the four cases; $\mu_m < 0$ and $\xi_m < 0$, $\mu_m < 0$ and $\xi_m > 0$, $\mu_m > 0$ and $\xi_m < 0$, or $\mu_m > 0$ and $\xi_m > 0$ can hold. Here we define the matrices $\mathbf{H}_m$ and $\boldsymbol{\Sigma}_m$ for the case $\mu_m < 0$ and $\xi_m < 0$. The other three cases can be derived similarly.

$$\mathbf{H}_m \equiv \begin{pmatrix} D_m & \underline{\mathrm{E}}_m & & & \\ & \ddots & \ddots & & \\ & & D_m & \underline{\mathrm{E}}_m & \\ & & & D_m & S \\ & & & & S \end{pmatrix} \in \mathbb{R}^{(Nx+1)(Ny+1)\times(Nx+1)(Ny+1)},$$

with

$$D_m \equiv \begin{pmatrix} d & \bar{e} & & \\ & \ddots & \ddots & \\ & & d & \bar{e} \\ & & & 1 \end{pmatrix} \in \mathbb{R}^{(Nx+1)\times(Ny+1)},$$

$$\underline{\mathrm{E}}_m \equiv \begin{pmatrix} \underline{\mathrm{e}} & e & & \\ & \ddots & \ddots & \\ & & \underline{\mathrm{e}} & e \\ & & & 1 \end{pmatrix} \in \mathbb{R}^{(Nx+1)\times(Ny+1)},$$

$$\text{and} \qquad S \equiv \begin{pmatrix} 1 & 1 & & \\ & \ddots & \ddots & \\ & & 1 & 1 \\ & & & 1 \end{pmatrix} \in \mathbb{R}^{(Nx+1)\times(Ny+1)}.$$

$$\mathbf{\Sigma}_m \equiv \begin{pmatrix} \Sigma_{m,\frac{1}{2}} & & & \\ & \ddots & & \\ & & \Sigma_{m,Ny-\frac{1}{2}} & \\ & & & \mathbf{0} \end{pmatrix} \in \mathbb{R}^{(Nx+1)(Ny+1)\times NxNy}, \qquad \text{with}$$

$$\Sigma_{m,j} \equiv \begin{pmatrix} \frac{\sigma_{i+\frac{1}{2}j+\frac{1}{2}}+\kappa_{i+\frac{1}{2}j+\frac{1}{2}}}{4} & & & \\ & \ddots & & \\ & & \frac{\sigma_{i+\frac{1}{2}j+\frac{1}{2}}+\kappa_{i+\frac{1}{2}j+\frac{1}{2}}}{4} & \\ & & & 0 \end{pmatrix} \in \mathbb{R}^{(Nx+1)\times Ny}.$$

With these definitions, the equation (3.4) can be written in the unknowns $\mathbf{\Psi}$ and $\mathbf{\Phi}$ as

$$\left(\begin{array}{ccc|c} \mathbf{H}_1 & & & -\Sigma_1 \\ & \ddots & & \vdots \\ & & \mathbf{H}_M & -\Sigma_M \\ \hline -\omega_1\mathbf{S} & \dots & -\omega_M\mathbf{S} & \mathbf{I} \end{array}\right)\left(\begin{array}{c} \mathbf{\Psi}_1 \\ \vdots \\ \mathbf{\Psi}_M \\ \hline \mathbf{\Phi} \end{array}\right) = \left(\begin{array}{c} \mathbf{Q}_1 \\ \vdots \\ \mathbf{Q}_M \\ \hline \mathbf{0} \end{array}\right), \tag{3.7}$$

where $\mathbf{I}$ is the $Nx \times Ny$ identity matrix and $\mathbf{0}$ is the Nx null vector. The usual technique to solve the equation (3.7), is to eliminate the angular flux $\mathbf{\Psi}_1, \dots, \mathbf{\Psi}_M$ using the Gaussian elimination. Therefore the storage requirements is reduced and the resulting equation

$$\left(\mathbf{I} - \frac{1}{4\pi}\sum_{k=1}^{M} w_k \mathbf{S}\mathbf{H}_k^{-1}\mathbf{\Sigma}_k\right)\mathbf{\Phi} = \frac{1}{4\pi}\sum_{k=1}^{M} w_k \mathbf{S}\mathbf{H}_k^{-1}\mathbf{Q}_k, \tag{3.8}$$

is solved for the scalar flux $\mathbf{\Phi}$, which does not depend on direction variables.

The source iteration method and synthetic-diffusion acceleration are among the most popular techniques used in computational radiative transfer. Most recently, a class of multilevel iterative solvers have been developed and experimented in [18, 20, 19] for radiative transfer in participating media. All the results given through the paper were obtained with the GMRES algorithm the linear system (3.8) to be solved for the mean intensity R only. For a detailed formulation of this algorithm in both two and three space dimensions we refer the reader to [18, 20] and [19], respectively.

4 Computational Results

We present numerical results for two test examples on optimal control problems in two space dimensions. The first example considers the radiant source as a control variable, while the mean intensity is taken as control variable in the second example. In all the results shown in this section, the S_8-discrete ordinates set is used for the angle discretization in radiative transfer equation and its associated adjoint problem. We use constant boundary data $A = 0$ for all test cases. For the optimization we start with the initial guess $Q^0(\mathbf{x}) = 0$ for all $\mathbf{x} \in D$. Furthermore, the steplength δ in (3.2) is chosen accordingly to the Armijo rule [21].

4.1 Example 1 (Source Inversion)

The first test-case is a source inversion problem. The computational domain is $D = [0,1] \times [0,1]$ discretized in 81×81 control volumes. The scattering and absorption coefficients are $\sigma = \kappa = 1$.

We set the desired source $\bar{Q}$ to be the sum of three Gaussian centered at $(1/4, 3/4)$, $(1/4, 1/4)$ and $(3/4, 1/4)$, respectively, i.e.,

$$\bar{Q}(x,y) = \frac{1}{\sqrt{2}} \sum_{i=1}^{3} e^{-\frac{(x-\bar{x}_i)^2+(y-\bar{y}_i)^2}{2}}.$$

We solve the transport equation with source $\bar{Q}$ to obtain $\bar{R}$. Then we consider the source inversion problem,

$$\min \frac{\alpha_1}{2} \int_D \left(R - \bar{R}\right) dx + \frac{\alpha_2}{2} \int_D Q^2 dx. \tag{4.1}$$

We stop the optimization if the relative difference in the functional is less than 10^{-6}. Plots of the contour lines of $R(\mathbf{x})$ and $Q(\mathbf{x})$ after the optimization can be found in the Figures 4.1-4.4. We observe that the position and strength of the placed sources could be retained by solving the optimization problem (4.1). We present results for different values of α_1 and α_2. In the Figures 4.1-4.2 we have a ratio $\alpha_1/\alpha_2 = 100$. The descent algorithm takes 18 gradient steps and an average of 4.16 functional evaluations per gradient step to reach the desired tolerance. The detailed history of the optimization is given in Table 4.1. The results of the Figures 4.3-4.4 are obtained for $\alpha_1/\alpha_2 = 1000$. Here the descent method takes 64 gradient steps with average of 3 functional evaluations per descent step. Hence the total number of functional evaluations doubles as soon as the problem loses its convexity properties. The history is similar to Table 4.1 and omitted.

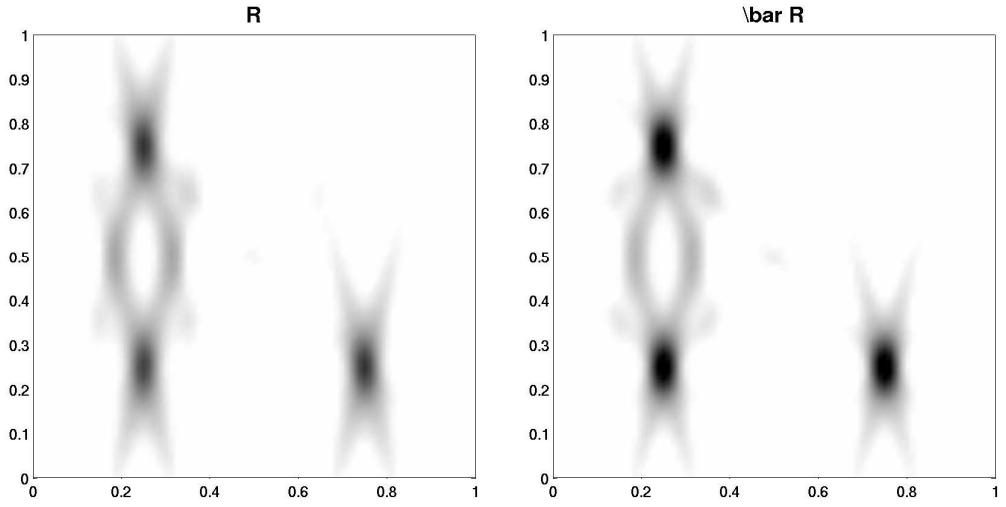

Figure 4.1: Corresponding radiative flux R for the control Q after optimization (left) and radiative flux $\bar{R}$ of the desired control $\bar{Q}$ (right). The weights are $\alpha_1 = 10^3$ and $\alpha_2 = 10$.

4.2 Example 2 (Edging)

We start with a given pattern $\bar{R}$ and ask for an energy distribution (source term) Q generating $\bar{R}$. For instance a laser beam might deploy the energy Q in the domain D to generate the desired pattern. Again, we compute the location of the source Q by solving (4.1). We

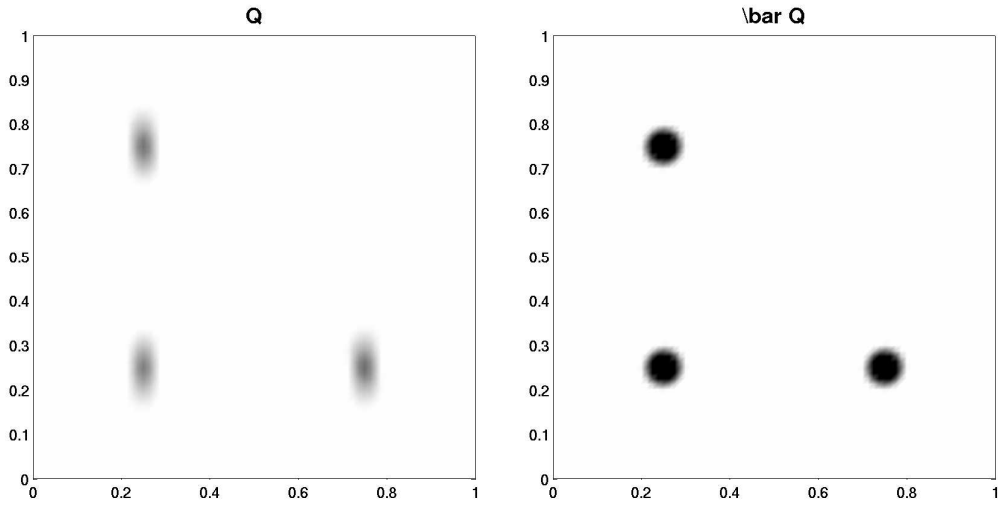

Figure 4.2: Sources Q obtained by solving the optimization problem (4.1) and original source $\bar{Q}$. The weights are $\alpha_1 = 10^3$ and $\alpha_2 = 10$.

prescribe a star-shaped pattern $\bar{R}$ as indicated in Figure 4.5. Contour lines of the solution to the optimization problem can be found in Figures 4.6-4.7. The parameters for this problem are $\sigma = 100$ and $\kappa = 1$. The grid is 81×81 and we compare different ratios α_1/α_2. The descent method always starts with $Q^0(\mathbf{x}) = 0$ in D. In Figure 4.6 we set $\alpha_1/\alpha_2 = 10$. It takes 30 gradient steps to reach the desired tolerance with an average of 3.1 functional evaluations per each descent step. In Figure 4.7 we set $\alpha_1/\alpha_2 = 1000$. Now the descent method takes 48 steps with an average of 6.3 functional evaluations per gradient step. Again we observe that the total number of functional evaluations increases as soon as the problem loses its convexity property. The optimal radiosity distribution shows in all cases the same star-shape pattern as the desired state.

5 Conclusions

We have presented an analytical and numerical study on optimal control problems of tracking type for RTE. Based on the adjoint calculus we derived the first–order optimality condition and proved the existence of an unique optimal control. For the numerical study we devised a steepest descent method and proposed an appropriate discretization for the minimization. Numerical experiments in two space dimensional for the source inversion problem are presented for the first time. Further research will focus on the time dependent problem and on radiative heat transfer, which yields a nonlinear coupling with a heat equation.

Acknowledgments

This work has been supported by the Kaiserslautern Excellence Cluster *Dependable Adaptive Systems and Mathematical Modelling* and by the DFG via SFB 568 and project PI 408/3-1.

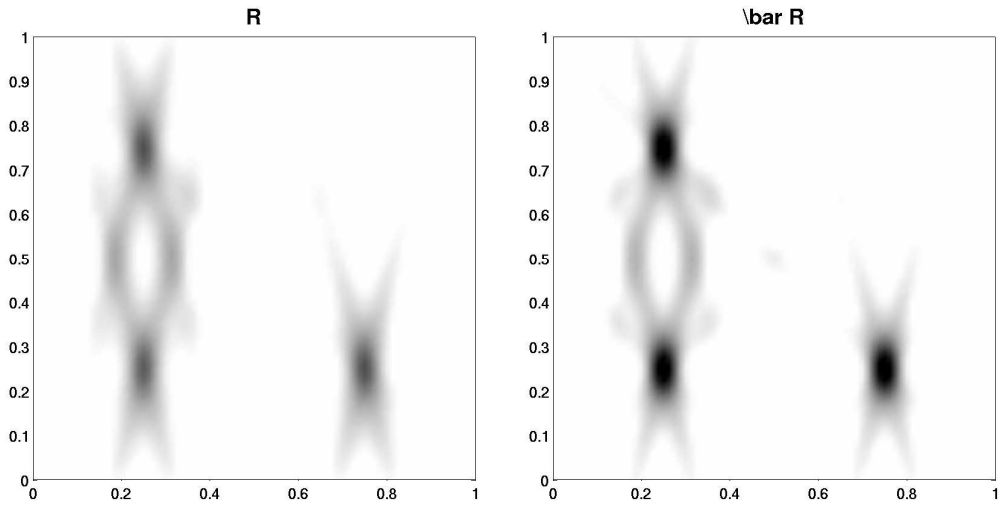

Figure 4.3: Corresponding radiative flux R for the control Q after optimization (left) and radiative flux $\bar{R}$ of the desired control $\bar{Q}$ (right). The weights are $\alpha_1 = 10^3$ and $\alpha_2 = 1$.

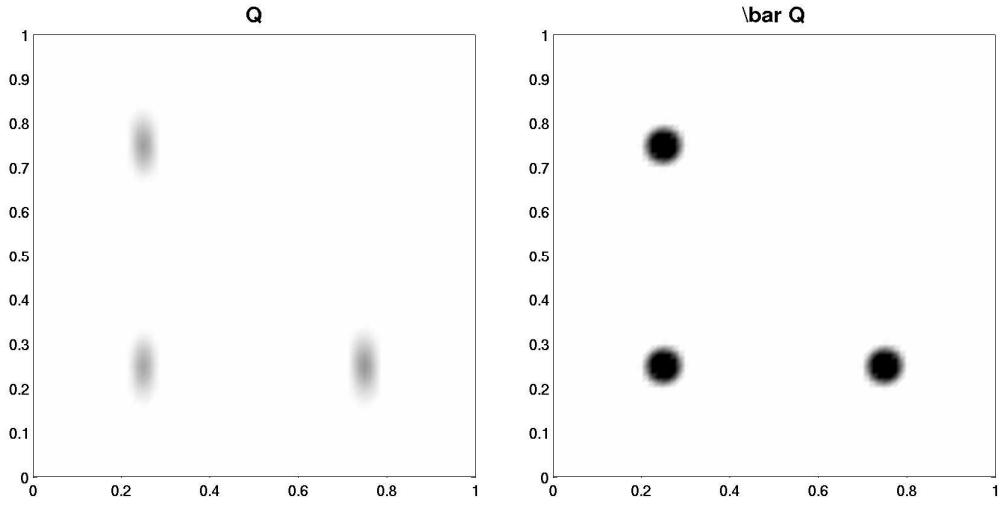

Figure 4.4: Sources Q obtained by solving the optimization problem (4.1) and original source $\bar{Q}$. The weights are $\alpha_1 = 10^3$ and $\alpha_2 = 1$.

# Iteration	$\int_D Q^2 d\mathbf{x}$	$\int_D (R-\bar{R})^2 d\mathbf{x}$	# Funct. eval.
1	0	1.3551e-003	5
2	3.7476e-005	4.9534e-004	4
3	3.7899e-005	3.5740e-004	5
4	6.0886e-005	2.4621e-004	3
5	8.8711e-005	2.0483e-004	5
6	1.0887e-004	1.3709e-004	4
7	1.1444e-004	1.2272e-004	4
8	1.3672e-004	1.1630e-004	5
9	1.3407e-004	9.6782e-005	3
10	1.6366e-004	8.8055e-005	5
11	1.6104e-004	7.3293e-005	3
12	1.8651e-004	6.9475e-005	5
13	1.8414e-004	5.7925e-005	3
14	2.0674e-004	5.6220e-005	5
15	2.0464e-004	4.7040e-005	3
16	2.2494e-004	4.6318e-005	5
17	2.2309e-004	3.8958e-005	3
18	2.4147e-004	3.8704e-005	5

Table 4.1: History of the optimization process. Iteration number versus residual and number of functional evaluations in the Armijo stepsize rule

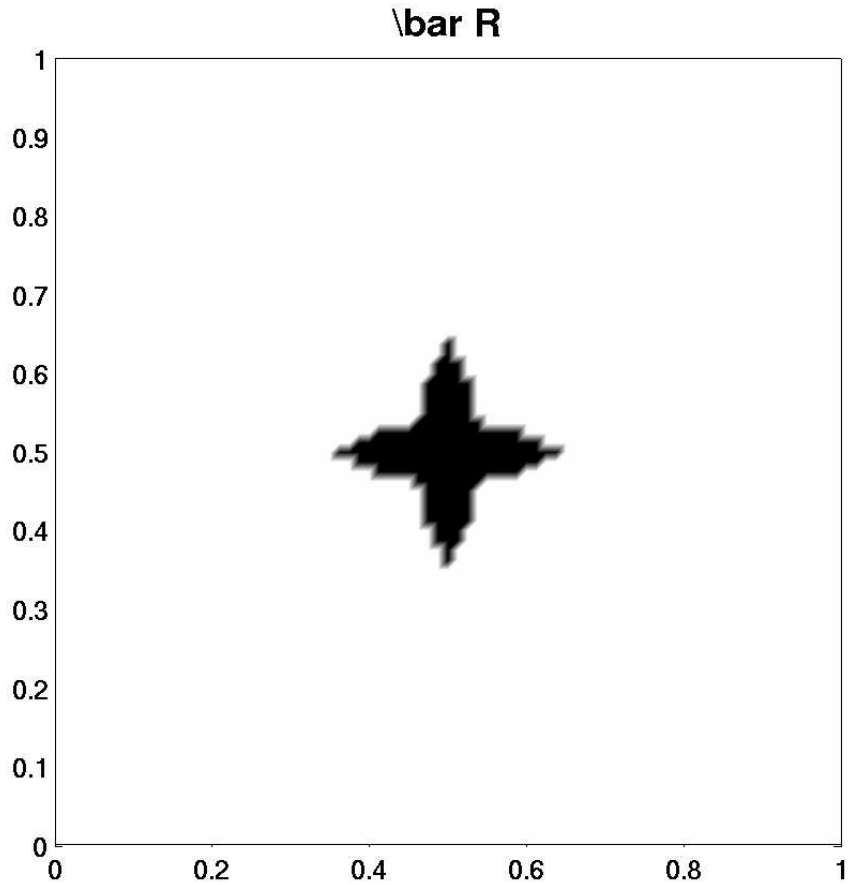

Figure 4.5: Contour line of the desired pattern $\bar{R}$.

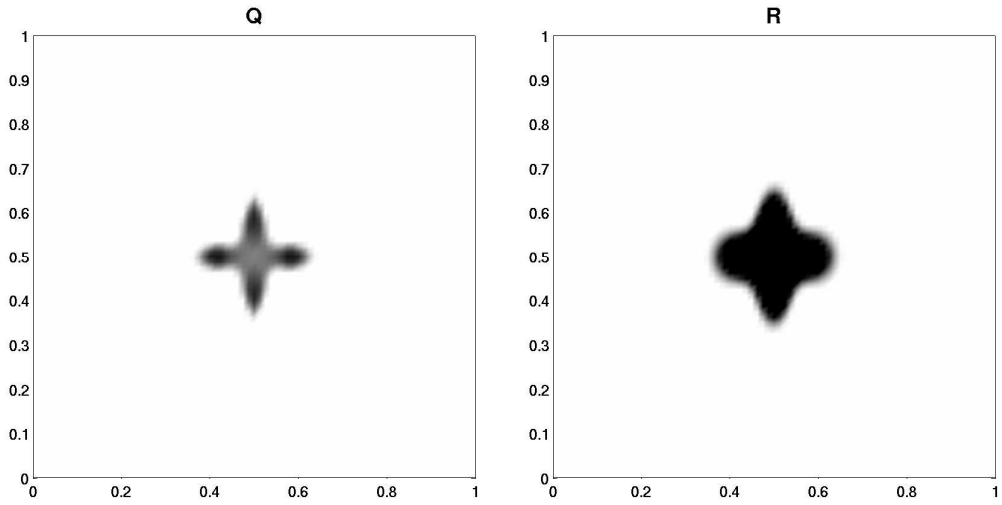

Figure 4.6: Contour lines of the optimal source distribution Q and the corresponding radiosity R. Weights applied are $\alpha_1 = 10^2$ and $\alpha_2 = 10$.

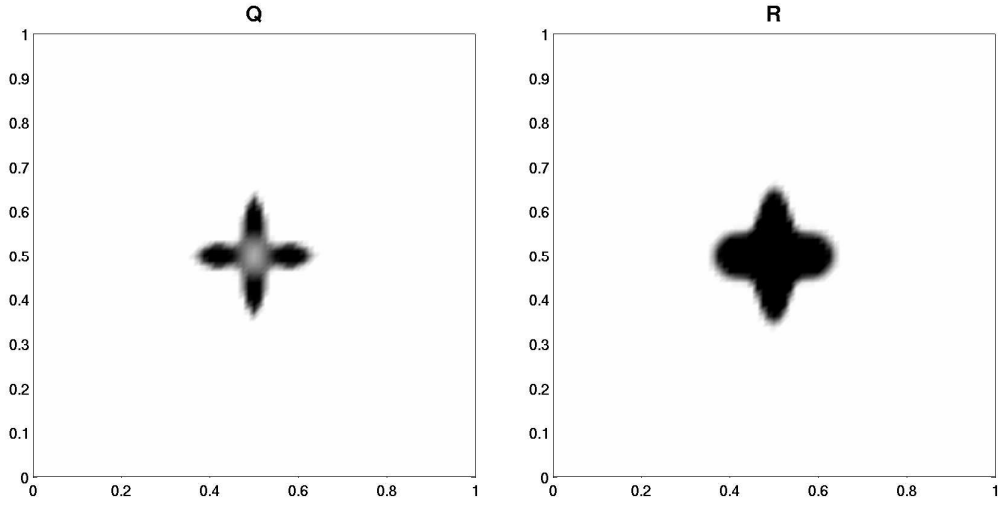

Figure 4.7: Contour lines of the optimal source distribution Q and the corresponding radiosity R. Weights applied are $\alpha_1 = 10^3$ and $\alpha_2 = 1$.

References

[1] V. I. Agoshkov, C. Bardos, *Optimal Control Approach in Inverse Radiative Heat Transfer Problems: The Problem of the Boundary Function*, **5**, ESAIM: Control Optimisation and Calculus of Variations, pp. 259-278, (2000)

[2] J.F. Bonnans, J.C. Gilbert, C. Lemarechal, C.A. Sagastizabal, *Numerical Optimization - Theoretical and Practical Aspects*, Springer (2002).

[3] J. M. Banoczi, C. T. Kelley, *A Fast Multilevel Algorithm for the Solution of Nonlinear Systems of Conductive-Radiative Heat Transfer Equations in Two Space Dimensions*, **20**, SIAM J. Sci. Comp., pp. 1214–1228, (1999)

[4] M. K. Choudhary and N. T. Huff. *Mathematical modeling in the glass industry: An overview of status and needs.* Glastech. Ber. Glass Sci. Technol., 70:363–370, 1997.

[5] W. Fiveland, *Discrete-Ordinates Solutions of the Radiative Transport Equation for Rectangular Enclosures*, J. Heat Transfer, **106**, pp 699-706, 1984

[6] A. R. Conn, N. I. M. Gould, P. L. Toint, *Trust-Region Methods*, MPS/SIAM Series on Optimization, SIAM Philadelphia (2000)

[7] M. T. Laitinen and T. Tiihonen, *Integro-differential equation modelling heat transfer in conduction, radiating and semitransparent materials*, Mathematical Methods in Applied Sciences, **21**, pp 375, 1998

[8] C. T. Kelley, *Existence and uniqueness of solutions of nonlinear systems of conductive-radiative heat transfer equations*, Trans. Theory and Statistical Physics, **25**, pp. 249–260, (1996)

[9] E.W. Larsen, G. Thömmes, A. Klar, M. Seaïd, and T. Götz. *Simplified P_n approximations to the equations of radiative heat transfer in glass.* J. Comp. Phys., 183:652–675, 2002.

[10] D. Levermore. *Moment closure hirarchies for kinetic theories.* J. Stat. Phys., 83, 1996.

[11] D. G. Luenberger, *Optimization by Vector Space Methods.*, John Wiley & Sons, New York, 1969

[12] S. Manservisi, K. Heusermann, *On some optimal control problems for the heat radiative transfer equation*, **5**, ESAIM: Control, Optimisation and Calculus of Variations, pp 425-444, (2000)

[13] D. Mihalas and B. S. Mihalas, *Foundations of Radiation Hydrodynamics.* Oxford University Press, New York, 1983.

[14] M. F. Modest, *Radiative Heat Transfer.* McGraw-Hill, 1993.

[15] S.S. Pereverzyev, R. Pinnau and N. Siedow. *Initial temperature reconstruction for a nonlinear heat equation: application to radiative and conductive heat transfer.* D. Lesnic (ed.), Proceedings of the 5th International Conference on Inverse Problems in Engineering: Theory and Practice, Cambridge. Leeds University Press 2005. Vol. III, ch. P02, pp.1-8.

[16] R. Pinnau, A. Schulze. *Newton's Method for Optimal Temperature-Tracking of Glass Cooling Processes.* Submitted for publication, 2004.

[17] R. Pinnau and G. Thömmes. *Optimal boundary control of glass cooling processes.* M2AS, 120:1261, 2004.

[18] M. Seaïd and A. Klar, *Efficient Preconditioning of Linear Systems Arising from the Discretization of Radiative Transfer Equation*, Lecture Notes in Computational Science and Engineering, **35**, pp 211-236, 2003

[19] M. Seaïd, M. Frank, A. Klar, R. Pinnau and G. Thömmes, *Efficient Numerical Methods for Radiation in Gas Turbines*, J. Comp. Applied Math., **170**, pp 217-239, 2004

[20] M. Seaïd, A. Klar and R. Pinnau, *Numerical Solvers for Radiation and Conduction in High Temperature Gas Flows*, Flow, Turbulence and Combustion, **3**, pp 413-432, 2005

[21] P. Spellucci, *Numerische Verfahren der nichtlinearen Optimierung*, Birkhäuser Verlag, Basel, (1993)

[22] P. Spellucci, *Nonlinear (local) optimization - the state of the art*, preprint, (2001)

[23] G. Thömmes, R. Pinnau, M. Seaid, T. Götz, and A. Klar. *Numerical methods and optimal control for glass cooling processes.* TTSP, 31(4-6):513–529, 2002.